FERMILAB-CONF-08-375-CD

OPTIMIZING CAVITY GRADIENTS IN PULSED LINACS USING THE CAVITY TRANSIENT RESPONSE*

G. Cancelo#, A. Vignoni, Fermi National Accelerator Laboratory, Batavia, IL 60510, U.S.A.

Abstract

In order to achieve beam intensity and luminosity requirements, pulsed LINAC accelerators have stringent requirements on the amplitude and phase of RF cavity gradients. The amplitude and phase of the RF cavity gradients under heavy beam loading must be kept constant within a fraction of a % and a fraction of a degree respectively. The current paper develops a theoretical method to calculate RF parameters that optimize cavity gradients in multi cavity RF units under heavy beam loading. The theory is tested with a simulation example.

INTRODUCTION

Modern pulsed LINAC accelerators are being designed taking advantage of the cost reduction that can be achieved powering a string of cavities from one klystron. At 70% peek power utilization a 10 MW klystron can power 24 superconducting cavities at an average gradient of 31.5MV/m and a beam current of 9mA. The XFEL main LINAC klystrons at DESY will power 32 cavities at 23.6MV/m and an average beam current of 5mA. As multiple cavities are connected to a single klystron the RF system parameters and control become more complex. A typical low level RF (LLRF) control loop controls the amplitude and the phase of the klystron's RF power, however, the loop cannot dynamically control individual cavity amplitude and phases. Typically, the control is done over the vector sum of all cavity gradients within the RF unit. The problem is further complicated by the need to obtain the maximum possible acceleration from the RF unit, pushing cavity gradients up close to their quenching limits. These cavity maximum gradients are different within a certain spread. Proton LINACs such as HINS [5] and Project X [6] add extra complexity to the RF system. A RF unit may need cavities operating at different synchronous phases (Φs). Secondly, particles travel cavities at increasing (non-relativistic) velocities, which implies different beam loading conditions from cavity to cavity.

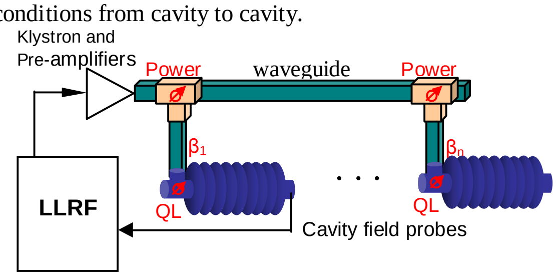

Figure 1.

Most of the literature available on cavity field dynamics follows a steady state approach [1-4]. The cavity is modeled by a 2nd order ODE (ordinary differential equation) and later approximated by a 1st order ODE model due to the high loaded Q of the cavity. The steady state approach determines optimality conditions for minimum generator power as a function of the cavity coupling parameter βopt and cavity tuning angle φ_{opt}. The steady state analysis works well for continuous waveform (CW) machines. A similar steady state assumption is assumed about the beam, and these models use the average beam current.

The steady state analysis applied to pulsed RF Linacs does not provide optimum operation parameters for all cases. For cavities operating "on crest" (Φs=0) under heavy beam loading and strong RF coupling an exact calculation of the forward power and beam injection time can set constant cavity gradients (flattops) and minimize or zero out the reflected power. For "on crest" operation, gradient flattops can still be maintained for cavities operating at different gradients with one time optimization of the coupling parameter. Unfortunately, this is not longer valid when cavities in the same RF unit need to be operated at different synchronous phases. Moreover, as is the case for pulsed RF proton beam Linacs such as HINS [5] and Project X [6], cavities have different beam loading conditions. To exemplify the theory that will be developed in this paper we use one RF unit from the Project X proposal. The RF unit has 3 cryomodules with a total of 21 cavities operating with synchronous phases and beam loadings as described in Table 1. A typical ±10% Vcav spread is assumed.

Table 1.

Cavity Number	Beam Beta In	Beam Beta Out	Cavity Phase (degrees)	Cavity voltage (MV/m)
182	0.9196	0.9208	-20	23.22
183	0.9208	0.9220	-20	25.62
184	0.9220	0.9232	-20	24.90
185	0.9232	0.9243	-20	27.30
186	0.9243	0.9255	-20	23.46
187	0.9255	0.9266	-19	26.34
188	0.9266	0.9277	-19	24.66
189	0.9277	0.9288	-19	24.18
190	0.9288	0.9299	-19	26.58
191	0.9299	0.9309	-19	22.74
192	0.9309	0.9320	-18	27.54
193	0.9320	0.9330	-18	25.38
194	0.9330	0.9340	-18	24.42
195	0.9340	0.9350	-18	26.82
196	0.9350	0.9360	-18	25.86
197	0.9360	0.9370	-17	22.98
198	0.9370	0.9380	-17	23.94
199	0.9380	0.9389	-17	25.14
200	0.9389	0.9398	-17	23.70
201	0.9398	0.9407	-17	26.10
202	0.9407	0.9416	-16	27.06

The steady state optimization minimizes the klystron reflected power during beam-on time using [1-4]:

$$\beta_{opt} = 1 + \frac{2RI_{b0}}{V_{cav}}\cos\phi_s \qquad \text{and} \qquad \varphi_{opt} = -\phi_s$$

Table 2 introduces the RF system parameters. For a description of these parameters see [1-4];

*Work supported by Fermi Research Alliance, LLC. under Contract No. DE-AC02-07CH11359 with the United States Department of Energy.
#cancelo@fnal.gov

Table 2.

Symbol	Definition
β	RF Coupling coefficient
Δω	Cavity detuning
ω_{12}	Cavity half bandwidth
R	Cavity shunt impedance
R_L	Loaded resistance
Ig	Generator current
Ib	Beam current
θ	Generator current phase

A simulation of the steady state optimum parameters using the RF unit example described above gives gradients and powers as shown in Figure 1. The simulator used is based on the 1st order dynamic models described in [1-4]. Also a ±10% uniformly distributed maximum cavity gradient spread has been assumed around the required average cavity gradient for the RF unit. We observe that although the reflected power is small the individual cavity amplitudes and phases are neither constant nor close to the set-point values. Also the vectorsum (Fig.1a black trace) is far away from the vectorsum set-point (Fig.1a blue trace). As a consequence, when the feedback loop is closed the individual cavity gradients are further distorted to accommodate the vectorsum to the setpoint. The LLRF closed loop is unable to control cavity voltages to individual set-points because the system is uncontrollable at the individual set point level.

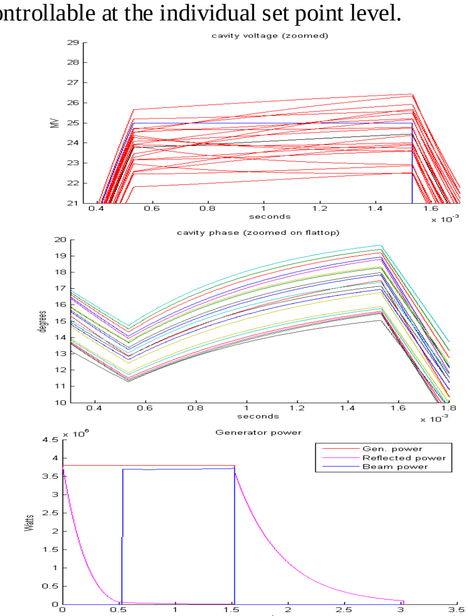

Figure 2 a) Cavity, vectorsum and vectorsum setpoint amplitude voltages, b) cavity phases, c) RF forward, reflected and beam powers.

TRANSIENT ANALYSIS

The RF system voltages and currents are modeled by

$$V(t) = V_A(t)\cdot e^{(j\omega + \phi(t))} = (V_r(t) + jV_i(t))\cdot e^{j\omega} \quad (1)$$

$$I(t) = I_A(t)\cdot e^{(j\omega + \phi(t))} = (I_r(t) + jI_i(t))\cdot e^{j\omega}$$

The RF voltages and currents in (1) are modulated in amplitude and phase. The LLRF controls the slow dynamics of the RF amplitude and phase called the RF envelope. The RF envelope is typically modeled by a 1st order ODE in the complex space C^1 [4].

$$\dot{V}_{cav}(t) = AV_{cav}(t) + BI_{tot}(t), \qquad (2)$$

As said, V and I are complex numbers, and

$$A = \begin{pmatrix} -\omega_{12} & -\Delta\omega \\ \Delta\omega & -\omega_{12} \end{pmatrix}, \qquad B = \begin{pmatrix} R_L\omega_{12} & 0 \\ 0 & R_L\omega_{12} \end{pmatrix}$$

Since the system is linear, the cavity voltage is the superposition of the cavity response to the generator and beam currents (power) $I_g e^{j\theta}$ and $I_b e^{j\pi}$. The current equations assume the convention that the phase is zero for the negative of the beam current.

The solution to equation (2) is given by:

$$\begin{aligned}\begin{pmatrix} V_r \\ V_i \end{pmatrix} = \frac{\omega_{12}R_L}{\omega_{12}^2+\Delta\omega^2}\Bigg\{ & e^{-\omega_{12}t} I_g \begin{pmatrix} -\omega_{12}\cos(\Delta\omega t+\theta)+\Delta\omega\sin(\Delta\omega t+\theta) \\ -\Delta\omega\cos(\Delta\omega t+\theta)-\omega_{12}\sin(\Delta\omega t+\theta) \end{pmatrix} u(t) + I_g \begin{pmatrix} \omega_{12}\cos\theta-\Delta\omega\sin\theta \\ \Delta\omega\cos\theta+\omega_{12}\sin\theta \end{pmatrix} u(t) - \\ & e^{-\omega_{12}(t-t_o)} I_b \begin{pmatrix} -\omega_{12}\cos\Delta\omega(t-t_o)+\Delta\omega\sin\Delta\omega(t-t_o) \\ -\Delta\omega\cos\Delta\omega(t-t_o)-\omega_{12}\sin\Delta\omega(t-t_o) \end{pmatrix} u(t-t_0) - I_b \begin{pmatrix} \omega_{12} \\ \Delta\omega \end{pmatrix} u(t-t_0) \Bigg\}\end{aligned} \qquad (3)$$

Where u(t) is the Heaviside function (i.e. u(t)=1 t≥0 and 0 otherwise).

To obtain a flattop at the injection time $t=t_0$ we must eliminate the time dependency in equation (3). That is achieved by making

$$I_g = e^{\omega_{12}t_o} I_b \quad (4) \qquad \text{and} \qquad \Delta\omega = -\theta/t_0 \quad (5)$$

Equations (4) and (5) guarantee a flattop for $t \geq t_0$. The appropriate value for the flattop amplitude and phase can be obtained from equation (3) at $t=t_0$-. This is given by

$$\begin{pmatrix} V_r \\ V_i \end{pmatrix}_{t=t_o} = \frac{\omega_{12}R_L}{\omega_{12}^2+\Delta\omega^2}\left\{ e^{-\omega_{12}t_o} I_g \begin{pmatrix} -\omega_{12} \\ -\Delta\omega \end{pmatrix} + I_g \begin{pmatrix} \omega_{12}\cos\theta - \Delta\omega\sin\theta \\ \Delta\omega\cos\theta + \omega_{12}\sin\theta \end{pmatrix} \right\} \qquad (6)$$

Using the tuning angle equation $\tan\psi = \frac{\Delta\omega}{\omega_{12}}$, the complex cavity voltage in (6) can be by its amplitude and phase

$$|V_c| = \frac{R_L I_b}{1+\tan^2\psi}\sqrt{\left(-1+e^{\omega_{12}t_o}(\cos\theta - \tan\psi\sin\theta)\right)^2 + \ldots + \left(-\tan\psi + e^{\omega_{12}t_o}(\tan\psi\cos\theta + \sin\theta)\right)^2} \qquad (7)$$

$$\phi_s = \tan^{-1}\left(\frac{\tan\psi\cos\theta + \sin\theta - \tan\psi e^{-\omega_{12}t_o}}{\cos\theta - \tan\psi\sin\theta - e^{-\omega_{12}t_o}}\right) \qquad (8)$$

Equations (7) and (8) have 3 degrees of freedom in the RF system phase space θ (or ψ), β and t_0. Both R_L and the half bandwidth of the cavity ω_{12} are a function of β. In a multi cavity RF unit, individual cavity flattops can be set calculating individual cavity values θ_{cav} and β_{cav} that satisfy (7) and (8) with (constrains (4) and (5) for a given t_0. However, t_0, the beam-on time, is unique for the RF unit and constrains the generator (reflected) power. Hence, to minimize the overall power requirements in an N cavity RF unit a system of 2·N equations with 2·N+1 unknowns must be solved.

RF POWER OPTIMIZATION

The reflected power is given by

$$P_{ref} = P_{gen} - \frac{dW}{dt} - P_{beam} - P_{diss}, \quad \text{where}$$

P_{ref}: reflected power.
P_{gen}: generator power
P_{beam}: power transferred to the beam.
dW/dt: change of stored energy in the cavity.
P_{diss}: cavity cryogenic losses.

For superconducting cavities P_{diss} is very small compared to the other members and can be neglected. If (6) and (7) are able to achieve a good flattop then dW/dt is also very small. Then we can approximate $P_{ref} \approx P_{gen} - P_{beam}$ and the reflected power is given by the mismatch between the RF system characteristic impedance and the cavity-beam impedance reflected to the waveguide (Fig 2).

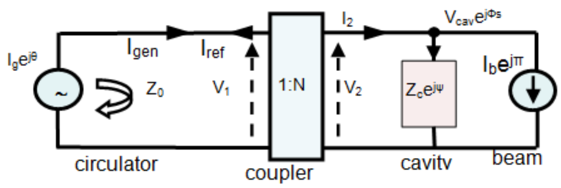

Figure 2

The cavity-beam impedance is given by the parallel

$$Z_{eq} = Z_{cav} // Z_{beam} = Z_c e^{j\psi} // \frac{V_{cav} e^{-j\phi_s}}{I_b} \qquad (9)$$

Minimizing the reflected power implies Z_{eq}/N^2 that should be a close match of Z_o. Given that Z_o is real, the imaginary part of Z_{eq} should be minimized and the real part of Z_{eq} reflected to the waveguide side should match Z_o.

OPTIMIZATION AND SIMULATION EXAMPLE

The nonlinear system given by (7), (8) and (9) with constrains given by (4) and (5) for each cavity can be solved to find an optimum set of parameters β_i^{opt}, ψ_i^{opt} (or θ_i^{opt}), and t_0^{opt}. As an example of the method described above we have used the same Project X RF unit described in Table I. The nonlinear system of equations has been solved using a numerical solver from Matlab. The optimized parameters were fed to the same RF unit simulator used to generate Figure 1. Figure 3 shows that the cavity gradients using the transient approach have been substantially improved both for amplitude and phase. This improvement to the individual cavity gradients is done at the cost of increasing the reflected power with respect to the steady state approach during the beam-on to about 4% of the beam power.

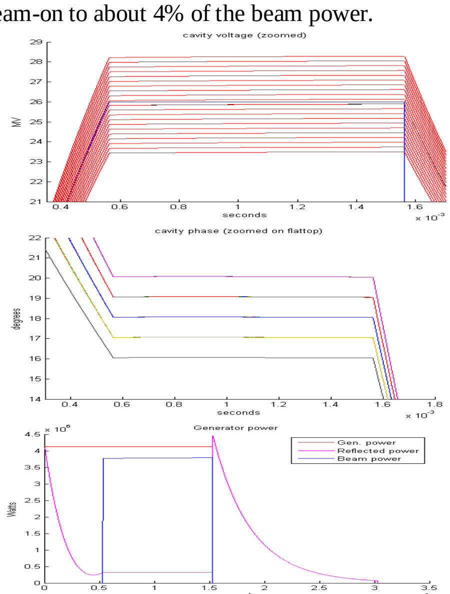

Figure 3 a) Cavity, vectorsum and vectorsum setpoint amplitude voltages, b) cavity phases, c) RF forward, reflected and beam powers.

CONCLUSIONS

The transient analysis allows optimum cavity gradient flattops across the RF unit, in particular when those cavities are operated at different synchronous phases (Φ_s) and with different beam loading conditions. The optimum RF parameters $\beta_i^{opt}, \psi_i^{opt}$ only need to be set once during the RF and beam commissioning and are not coupled with parameters in other cavities in the RF unit. The beam-on time t_0^{opt} can be used to minimize the RF generator power. For the sake of comparison Table 3 shows the optimization parameters obtained by each method.

Table 3.

Cavity Number	Steady state		Transient	
	Beta	Theta	Beta	Theta
182	2942	-20.00º	3473	-35.54º
183	2692	-20.00º	4184	-34.77º
184	2797	-20.00º	3881	-35.10º
185	2574	-20.00º	4540	-34.40º
186	3021	-20.00º	3257	-35.79º
187	2731	-19.00º	4109	-33.11º
188	2940	-19.00º	3515	-33.72º
189	3022	-19.00º	3292	-33.96º
190	2770	-19.00º	3993	-33.23º
191	3262	-19.00º	2663	-34.66º
192	2728	-18.00º	4151	-31.33º
193	2981	-18.00º	3439	-32.03º
194	3119	-18.00º	3071	-32.40º
195	2858	-18.00º	3781	-31.69º
196	2982	-18.00º	3436	-32.03º
197	3395	-17.00º	2398	-31.28º
198	3278	-17.00º	2691	-30.98º
199	3140	-17.00º	3049	-30.63º
200	3348	-17.00º	2516	-31.16º
201	3055	-17.00º	3272	-30.41º
202	2977	-16.00º	3515	-28.40º

REFERENCES

[1] Wilson, P.B. "High energy Linacs: Application to storage ring RF systems and linear colliders", SLAC-PUB-2884 Nov. 1987.

[2] Schilcher, T. "Vector Sum Control of Pulsed Accelerating Fields in Lorentz Force Detuned Superconducting Cavities", Ph.D thesis, DESY, Hamburg, August 1998.

[3] Padamsee, H., Knobloch, J., Hays, T., *RF Superconductivity for Accelerators*, John Willey & Sons, Inc., New York, 1998, p.381-401.

[4] T.P. Wangler. *Principles of RF Linear Accelerators*, John Wiley&Sons, Inc., NY, 1998.

[5] P.N. Ostroumov et al, "Front end design of a multi-GeV H-minus Linac", Proc. PAC-2005 (Knoxville, TN), 2005, ed. C. Horak p 3286.

[6] P.N. Ostroumov, "Physics Design of the 8-GeV H-minus Linac". New Journal of Physics, New J. Phys. **8** 281, 2006. http://stacks.iop.org/1367-2630/8/281